Techno-Economic Optimization of Grid-Integrated Hybrid Storage System using GA

Arafat Ibne Ikram
Dept. of Electrical and Electronic Engineering
International Islamic University Chittagong
Chattogram 4314, Bangladesh
arafatibne.ikram@gmail.com

Md. Sajjad-Ul Islam
Dept. of Electrical and Electronic Engineering
International Islamic University Chittagong
Chattogram 4314, Bangladesh
sajjadulislam714@gmail.com

Md. Arafat Bin Zafar
Dept. of Electrical and Electronic Engineering
International Islamic University Chittagong
Chattogram 4314, Bangladesh
arafatbzafar@gmail.com

Md. Kamruzzaman Rocky
Dept. of Electrical and Electronic Engineering
International Islamic University Chittagong
Chattogram 4314, Bangladesh
kamruzzamanrocky7@gmail.com

Imtiaz
Dept. of Electrical and Electronic Engineering
International Islamic University Chittagong
Chattogram 4314, Bangladesh
imtiazalam1300@gmail.com

Asif Rahman
Dept. of Electrical and Electronic Engineering
International Islamic University Chittagong
Chattogram 4314, Bangladesh
rahman.asif450@gmail.com

***Abstract*—Microgrids (MG) are innovative in lowering GHG emissions from electricity production by using renewable energy sources. The technical and economic feasibility of MG operation with hybrid energy storage systems is challenged by the intermittent nature of renewable generation. The hybrid energy storage system has been investigated for decades. We provide a hybrid energy storage system with a Grid-connected MG integration model to assess its technological, economic, and environmental impacts. The MG model included photovoltaic panels, wind turbines, lead-acid batteries, electrolyzer modules, fuel cells, and H_2 cylinder tanks. The mathematical function for each component used in the system is developed individually to estimate the annual hourly energy generation and consumption. Annual hourly data sets of load consumption are used as load models. The number of components needed for the MG operation to run economically feasible is achieved using the Genetic algorithm (GA) optimization technique thereafter reducing the Levelized cost of energy (LCOE) of the system. An energy dispatching technique is employed to efficiently distribute energy across the hybrid storage and load models. We examined different MG energy penetration levels of 25%, 50%, 75%, and 100% in terms of peak power distribution capacities to load demand relative to the existing grid. MG with 100% integration strives to maintain full load demand without buying energy from the grid. The LCOE and GHG emissions for each Grid-MG integration scenario are calculated. At 100% of the penetration scenario, the LCOE was found 0.0611 ($/kWh) which was best among all the other penetration scenarios.**

***Keywords*—Microgrid, Genetic algorithm, Generation, Hybrid energy storage, Sustainable energy, Energy management.**

I. Introduction

One of the most urgent problems facing the planet today is the impact of global warming. In many developing countries, rising carbon emissions and greenhouse gas levels are attributable to rapid industrialization and urbanization. Many areas are now unfit for commercial agriculture because of drought and sudden temperature increases. Soil conditions are more directly affected by land use and management than by the indirect effects of climate change, yet adaptive behavior may help mitigate these negative effects. Even if carbon dioxide production were to stop tomorrow, the climate would still shift [1]. Climate change, sea level rise, desertification, and erratic weather patterns may all be exacerbated by pollution and uncontrolled greenhouse gas emissions. Changing patterns of energy production, growth, and consumption may be seen in the emergence of new renewable technologies in developing countries. Potentially resolving a pressing environmental, social, and economic problem—global carbon emissions—through the effective use of solar PV panels and concentrated solar power plants is a distinct possibility [2].

The average atmospheric concentration of carbon dioxide in 2019 was $414,7ppm$, 45% more than between 1980 and 1990 [3]. Renewable energy reduces GHG emissions and combats climate change. The literature contains evaluations of optimization studies that took into account the accessibility of renewable resources and the regional electricity demand. The optimal sizing of energy storage in grid-connected mode and multi-operational management in hybrid systems are just two examples of many studies conducted on the topic of size optimization and energy management in hybrid renewable systems [4], [5]. In a size optimization strategy, the ideal proportions for each part are determined by analyzing how well they serve overarching goals. Many goals, including cost and dependability, could be expressed for a size optimization issue or challenge. The literature on hybrid system size optimization has addressed both single-objective and multi-objective frameworks. Optimization for a particular target, like size, has been the primary focus of previous studies.

Renewable energy is in high demand because of people's growing concern for the environment. A renewable energy system that is well-planned may reduce the cost and increase the efficiency of the power supply. Cutting down on the number of parts in a microgrid can save money and cut down on energy costs. We developed a model of a microgrid that operates inside an existing grid and used GA to optimize the model's techno-economic parameters and assess the system's environmental performance across a range of penetration rates. Hybrid renewable systems use conventional networks and other dispatchable energy sources to dampen the intermittent nature of renewable power output. The goal of this project is to build a grid-connected microgrid that can sell excess electrical energy to the conventional grid and buy energy from it when needed by utilizing primary generating units like solar photovoltaic panels and wind turbines, as well as energy storage systems that employ a mathematical method. The goal of this study is to apply a genetic algorithm (GA) to determine the optimal number of each component needed to build a renewable energy power plant that would be both cost-effective and environmentally friendly.

II. Modeling of Microgrid Systems

The proposed microgrid is comprised of solar PV panels, wind turbines, batteries, electrolyzers, fuel cells, and H_2 tank as shown in Fig. 1. Each of the components is designed with a respective mathematical model to calculate hourly generation or consumption by given resources.

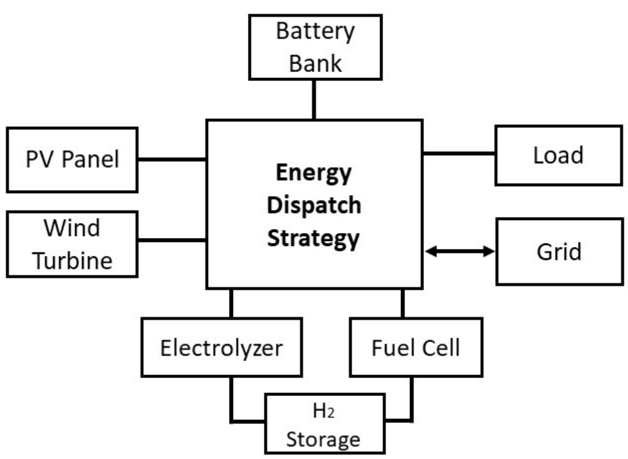

Fig. 1: Schematic Diagram of the System

We used an optimization method to reduce the levelized cost of energy and greenhouse gas emissions after implementing an Energy Dispatched Strategy. In this case, as shown in Fig. 1, both PV and WT were used as the principal renewable power sources. MG are energy distribution networks that link loads, the grid, and various forms of energy storage. EM and FC were linked up to the Hydrogen Storage system. Excess power may be utilized to charge the battery bank during times of high generation, and the battery bank can be replenished by purchasing power from the traditional grid during times of low generation.

A. Solar Photovoltaic Panel Model (PV)

The solar photovoltaic cell is basically a p-n junction semiconductor, whose photo-current is directly proportional to solar radiation, $DNI(t)$. The hourly energy generation by the PV panel can be obtained from the photo-current (I_{max}) shown in (1) [6].

$$I_{max}(t) = N_p I_{ph}(t) - N_p I_s(t) \times \left[\exp\left(q\Big(\frac{v}{N_s k T_c A}\Big) - 1 \right) \right] \tag{1}$$

PV panel hourly Energy generation P_{pv} was achieved using (2) [6].

$$E_{pv}(t) = V_{max}(t) \times I_{max}(t) = \gamma . V_{oc}(t) . I_{sc}(t) \tag{2}$$

Here, Band-gap energy of semiconductor, $E_g = 1.11eV$, charge of one electron, $q = 1.6 \times 10^{-19}C$ and Boltzmann's constant, $k = 1.38 \times 10^{-23} J/K$. Terminal voltage, V_{max}, and the ideal factor, $A = 1.3$.

B. Wind Turbine Model (WT)

The quadratic model of wind function was used to calculate the hourly output energy of a WT from hourly wind velocity, $V(t)$ which is shown in Equation (3).

$$E_{WT}(t) = \begin{cases} P_{WT}\Big(\frac{V(t) - V_{in}}{V_{rate} - V_{in}}\Big) \text{ for } V_{in} \leq V(t) \leq V_{rate} \\ P_{wt} \text{ for } V_{rate} < V(t) < V_{out} \\ 0 \text{ for } V(t) < V_{in} \text{ and } V(t) > V_{out} \end{cases} \tag{3}$$

Here, the Vestas 1kW WT model is assumed which has rated power $P_{wt} = 1000W$, rated wind speed $V_{rate} = 12m/s$, cut-in speed $V_{in} = 3m/s$ and cut-of speed $V_{out} = 23m/s$ [7].

C. Energy Storage System Modeling (BAT)

The amount of energy accessible in energy storage at a given moment is estimated using the following equation (4) [8].

$$SOC(t) = SOC(t-1) + \frac{\eta_{ch}(t).CH.\Delta t}{Bat_{cap}} + \frac{DCH(t).\Delta(t)}{\eta_{dch}.Bat_{cap}} \tag{4}$$

Here, BAT capacity $Bat_{cap} = 1000Ah$, BAT charging efficiency $\eta_{ch} = 80\%$, discharging efficiency $\eta_{dch} = 95\%$ and t is denoted as hourly representation.

D. Electrolyzer Module Modeling (EM)

The amount of hydrogen consumed by an EM per hour (3600 seconds) can be estimated using the equation (5) and (6).

$$\begin{aligned} H_{2_{Produced}}(t) &= \frac{I_{em} N_{em}}{2 \times F} \times \eta i \times 3600 \\ &= \frac{P_{em}(t)}{2 \times V_{em} \times F} \times 3600 \end{aligned} \tag{5}$$

$$P_{EM} = I_{em} \times V_{em} \quad \eta i = 1 \tag{6}$$

Here, Rated Power of the EM $P_{em} = 1000$, the working voltage $V_{em} = 2V$, and the electrical efficiency $\eta i = 74\%$ [9].

E. Fuel Cell Modeling (FC)

Total power generated by FC per hour (3600 seconds) can be estimated using the equation (7) and (8).

$$\begin{aligned} H_{2_{Consumed}}(t) &= \frac{I_{fc}N_{fc}}{2 \times F} \times \frac{1}{\mu_{fc}} \times 3600 \\ &= \frac{P_{fc}(t)}{2 \times V_{fc} \times F} \times 3600 \end{aligned} \tag{7}$$

$$P_{fc} = I_{fc} \times V_{fc} \tag{8}$$

Here, the rated power of FC $P_{fc} = 1kW$, faraday's efficiency $\mu_{fc} = 96487C$ [10], the working voltage $V_{fc} = 2V$, and the efficiency of FC $N_{fc} = 47\%$ [11].

III. Energy Management System

An energy dispatched system is proposed to smartly store the renewable energy in the hybrid energy storage and consumed at peak load hours. Every component of the microgrid is designed using a mathematical representation to calculate the hourly energy it may produce or consume. Solar PV panel and wind turbine models calculate the hourly generation from solar irradiance, temperature, and wind speed. By comparing hourly generation and consumption, the EMS algorithm determines whether it will store the energy or drain the energy storage. The algorithm tries to maintain the instantaneous SOC(t) of the battery between $20\% \leq SOC(t) \leq 90\%$. If the $SOC(t) \leq 90\%$ then excess energy is taken to the Electrolyzer terminal. Then H_2 tank capacity is checked for the availability of storing more hydrogen. If the H_2 is full, then excess energy is sold to the power grid, otherwise, when the demand is higher than the load demand, the algorithm first checks if the SOC is higher the 20%, if not, then the system will try to pull energy from fuel cell, which will consume hydrogen from the H_2 tank. If there is no H_2 gas left, then the algorithm will buy energy from the power grid. Selling on the grid is assumed 50% of the retail electricity price.

IV. Genetic Algorithm (GA

The genetic algorithm optimization technique is used to optimally size the capacity of the proposed MG model. The sole purpose of the optimization is to minimize the net present cost of the MG as well as lower the LCoE. So the correct sizing is required for minimizing the cost. GA is chosen for this particular problem of finding the optimal number of components needed for the system to run optimally. The algorithmic flowchart of GA is shown in Fig. 2. Firstly, sets of a number of components for PV, WT, BAT, EM, FC, EM, and H_2 tank were initially generated randomly with the constraint in mind. Then each set is tested against the objective function to find the minimal fitness among those initially generated populations, which is given in Equation (9). The penalty is given on the fitness function if it doesn't satisfy any constraints. After the first generation of offspring, the algorithm then puts all those firstly generated populations in Elitism, parent selection, cross-over, mutation, and finally generated the new population for the second iteration. After that, each population of this new population is again tested against the objective function to find its minimal value. If it cannot find a new best solution after the new offspring, it will consider the older best as the current best fitness. Otherwise, after passing the penalty function, if it finds minimal fitness compared to the previous, it will consider the newly achieved fitness as the best fitness. After each iteration of the algorithm, the constraint will check that it has not been so minimized for lowering the cost that it cannot satisfy the load demand.

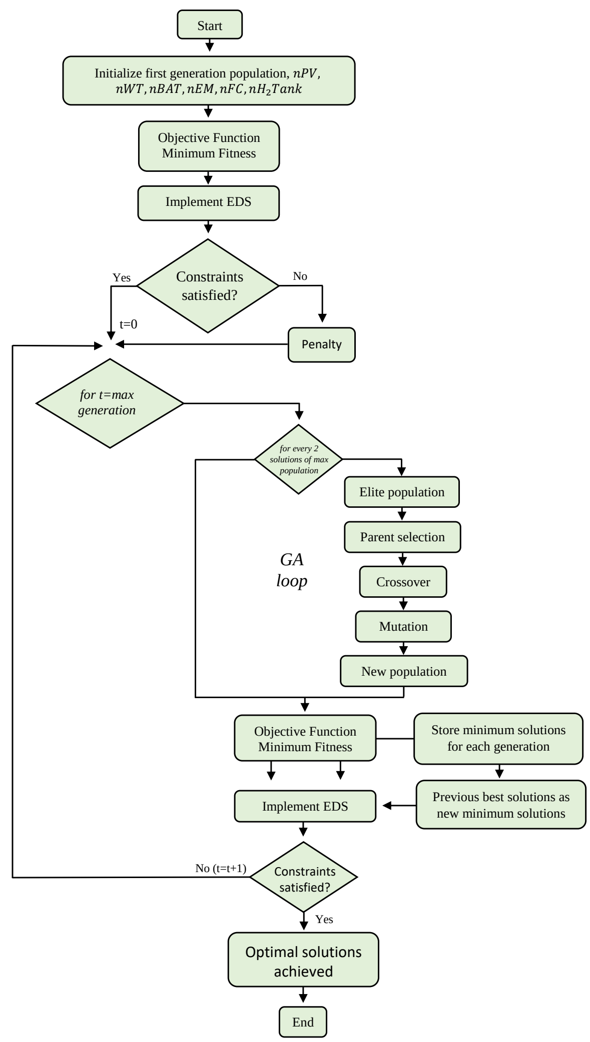

Fig. 2: Genetic algorithm optimization flowchart

The microgrid is tested against four different penetration levels with the power grid. These four penetration levels 25%, 50%,75%, and 100% are the main constraints of penalty checking. For 25% MG-Grid penetration, GA has bound the size of the microgrid to serve 25% of the total load demand from the proposed microgrid, other 75% will be bought from the existing power grid.

$$F(O) = min \sum_{n=1}^{n_{max}} NPC \tag{9}$$

The population size of 100 is considered the maximum of 1000 generations for the GA, where the minimum boundary is 0 and the maximum boundary is about 2000. The population of each set represents a configuration for a number of components used in the system.

V. Economic assessment model

LCOE for grid-connected MG is calculated using Equation (10) [12].

$$LCOE = \frac{CRF \times NPC + Grid_{Bought} - Grid_{Sell}}{\sum_{t=1}^{t_{max}=8760} Load(t)} \tag{10}$$

Here, $(Grid_{Bought})$, and $(Grid_{Sell})$ are the annual total power sold and Bought from the grid. $\sum_{t=1}^{t_{max}=8760} Load(t)$ is the total annual hourly energy consumption. The CRF is calculated using the equation (11) [12].

$$CRF = \frac{IR(1+IR)^T}{(1+IR)^T - 1} \tag{11}$$

Here, the interest rate $IR = 8\%$, Project lifetime $T = 25 year$. The total net present cost is estimated using the equation (12) [12].

$$NPC = \sum_{k_i}^{ki_{max}} (IC_k + MC_k + RC_k) \tag{12}$$

Here, The vector index of the component $ki =$ PV, WT, BAT, EM, FC, Tank. NPC is calculated for each component that is used in MG. The installation, maintenance, and replacement cost of each component were calculated using the equation (13), (14), and (15) respectively.

$$IC_k = (N_k \times CC) \tag{13}$$

$$MC_k = N_k \times K_{O\&M} \times \sum_{n=1}^{N} \left(\frac{1+ER}{1+IR}\right)^T \tag{14}$$

$$RC_k = N_k \times K_{RC} \times \sum_{n=5,10,15}^{N} \left(\frac{1+ER}{1+IR}\right)^T \tag{15}$$

Here, N is the number of components that are achieved from GA. $'K'$ is the type of component $i.e - PV,\ WT,\ EM,\ FC,\ BAT,\ H_2\ tank, and\ Inverter$. Escalation rate $ER = 5\%$.

TABLE I: Price Table of Microgrids Components [12], [13]

Components Name	Per Unit Capacity	CC ($)	O&M ($/W)	RC ($)	Lifetime (Years)
PV	0.435 kW	468	4.35	-	20
WT	1 kW	950	19	800	20
BAT	12kWh (12V, 1000 Ah)	350	-	300	10
Inverter	10kW	100 ($/kW)	-	-	10
EM	1kW	2000	10	1500	10
FC	1kW	3000	60	2500	15
H_2 Tank	6kg/Unit	3960	79.2	-	20

VI. Greenhouse gas emission estimation model

Greenhouse gas emissions occur during the life cycle stages of every component [14] even from the renewable generator. The life cycle assessment (LCA) of any component can be evaluated using the model shown in the equation (16).

$$Emission_{total} = \sum_{ki=1}^{ki=6} (TE_k \times \zeta_k) \tag{16}$$

Here, the annual total energy generation by each component is denoted as TE_k, and ζ is the emission factor which is given in Table II.

TABLE II: Emission Factor [14]

Item	PV	WT	BAT	EM	FC	Grid
Emission factor ζ $(KgCO2eq./kWh)$	0.045	0.01	0.028	0.011	0.15	0.1660

VII. Analysis Condition

A. Renewable resource data

Solar irradiance and wind speed data sets for Halishahar, Chittagong are gathered from the NASA Power tool which is shown in Fig. 3.

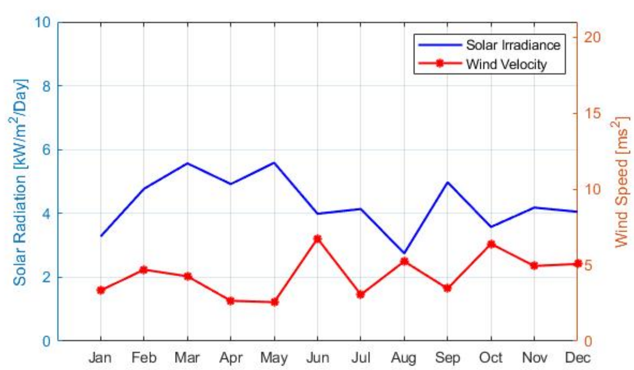

Fig. 3: Monthly Solar Irradiance and Wind Speed

Solar insolation of 4.862 $KW/m^2/day$ is radiated throughout the year. This has a very high potential for solar energy generation. Additionally, an average wind speed of 4.26 ms^2 is recorded annually, which is pretty insignificant for wind generation [15]. Annual data solar irradiation and wind speed data for the specified location is shown in Fig. 3.

B. Load Model

The annual hourly load consumption model is created to test renewable generation. For each month of the year same load curve is considered 1% varying load consumption. The hourly load curve was shown in Fig. 4.

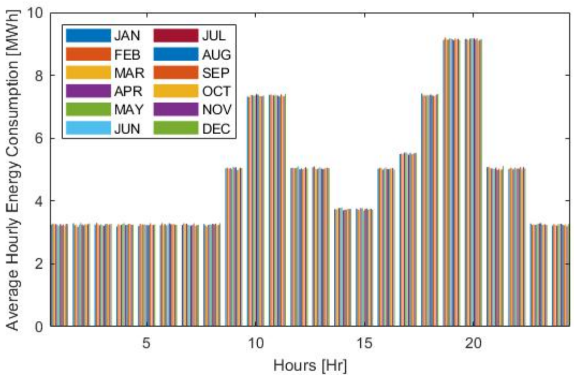

Fig. 4: Hourly load demand

VIII. Results & Discussions

The optimization is performed only with the intention of achieving the goal of reducing the net present cost as much as possible. The optimization convergence curve for a range of different penetration levels is depicted in Fig. 5. The evolutionary algorithm is applied to the problem of determining the optimal size of the MG that is connected to the larger grid, taking into account the economic viability of the system. Analyzing four different MG energy penetration scenarios allows for the calculation of the optimum size.

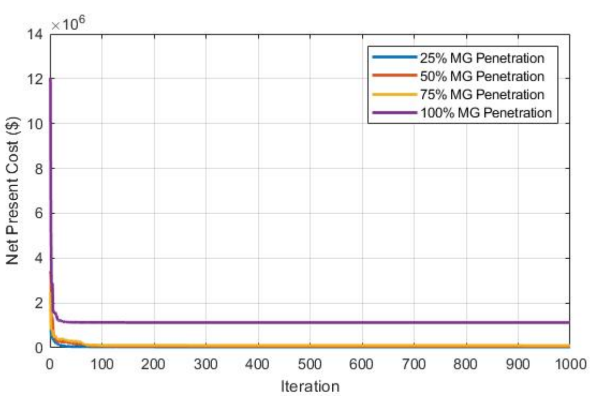

Fig. 5: Convergence curve for all MG penetration levels

Fig. 5 displays the output convergence curve of GA for microgrid energy penetration levels of 25%, 50%, 75%, and 100% respectively.

The LCOE is calculated for each of the MG penetration scenarios presented in Fig. 6, which were successively 25%, 50%, 75%, and 100% of the total grid. The lowest LCOE, is calculated to be 0.061 ($\$/kWh$) when applied to a scenario in which MG and the grid are both fully utilized. The lowest LCOE is found for the scenario in which 25% of the penetration is achieved.

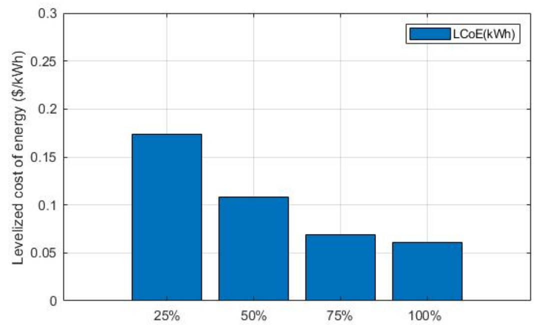

Fig. 6: LCOE for all penetration levels

The statistics for hourly renewable generation and load consumption of various components employed in the MG are displayed in Fig. 7 for scenarios with a penetration level of 100 percent on a monthly average scale. These are some data pertaining to the many different components that will be used in the MG. In order to arrive at this conclusion, we took into account not only the energy that was extracted from the battery but also the power that was produced by the fuel cell. When the level of penetration hits 100 percent, any excess energy that is produced by renewable sources is promptly deposited into an energy storage pack. This takes place when the level of penetration reaches one hundred percent. During periods when renewable forms of energy were not available, battery storage and fuel cell power plants were deployed to meet load requirements. The daily average load data is also plotted in Fig. 7. A portion of the extra power is sold back to the grid.

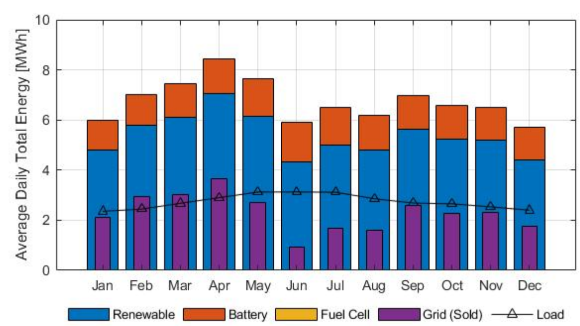

Fig. 7: Monthly avg. energy generation

The results of the optimization show that the CO_2 emissions were 25%, 50%, 75%, and 100%, respectively. The solar PV and the grid are both responsible for the CO_2 emissions that are created by this particular MG system, as established by the information that we currently possess. The quantity of CO_2 that our microgrid emits over the course of a single year is depicted in Fig. 8.

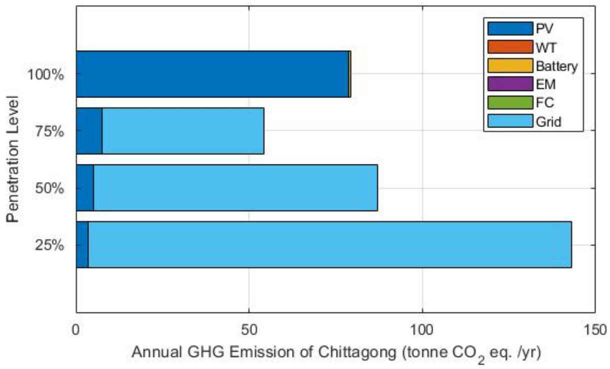

Fig. 8: GHG Emission

TABLE III: Techno-economic parameters for optimally designed MG

Type	Item	Penetration Level			
		25%	**50%**	**75%**	**100%**
Installed Capacity (KW)	PV	27	40.05	65.7	624.6
	WT	0	0	0	1
	BAT	0	0	0	533
	EM	1	1	1	1
	FC	1	1	3	1
	H_2	1	1	1	1
Annual Energy (MWh/yr)	Renewables	90.469	125.809	206.383	1963.533
	$Grid_{Sold}$	0.021	0.970	9.391	839.528
	$Grid_{Bought}$	843.996	497.316	227.541	0
Cost Analysis ($)	$Grid_{Revenue}$	2.171	97.076	676.252	83825.181
	$Grid_{Expense}$	167375.615	98983.806	55815.502	0
	NPC	81479.426	119841.632	171071.584	1806490.551
LCOE ($/KWh)		**0.173**	**0.108**	**0.068**	**0.0611**

The optimal sizing needed for the proposed system to run with the minimal operating cost is shown in Table III. Annual renewable generation and the transaction between grid and MG systems were also shown. Finally, The economic breakdown shows the upfront cost required for each system to run optimally, and the LCoE is also calculated for each penetration scenario and found to be the lowest of 0.0611 ($\$/kWh$) for the peak MG penetration.

IX. Conclusions

In this study, we have implemented the hybrid energy storage system in a grid-connected scenario. Here, we have done a comparative assessment of a grid-connected micro-grid system with energy penetration levels of 25%, 50%, 75%, and 100%. We demonstrated how the yearly energy production and economic cost effect of MG would change based on the amount of penetration of MG in the market at any given time. GA is used to determine the appropriate size of the MG, which allowed us to create the best possible configuration for the MG. The optimal quantity of the MG component would result in a significant reduction in the cost of installation as well as the LCOE. Following a series of experiments simulating various patterns of energy use, we determined that the LCOE ranges from $0.11 to $0.15 per kilowatt-hour. The lowest amount of LCOE is attained when the MG penetration level is 100. When it came to the cost of installation, however, the best results were obtained when the penetration cost is at its lowest possible level. The yearly Greenhouse Gas emission is determined to be lowest on the MG 100 energy penetration level scenario, where the principal generator source is the RES. As a result, it left a less carbon footprint when taking the LCA of DG's into consideration.

An extensive search for renewable energy sources and environmentally friendly energy storage has been ongoing as the world's supply of fossil fuels has been rapidly depleting and its emissions of greenhouse gases have been rapidly increasing. This study looked into the impact that different system architectures and energy storage methods have on LCOE and LCA. If necessary, a cost-benefit analysis of various energy storage options could be carried out. And we were able to get a good overall picture of the system.

References

[1] K. O. Yoro and M. O. Daramola, "Co2 emission sources, greenhouse gases, and the global warming effect," in *Advances in carbon capture*. Elsevier, 2020, pp. 3–28.

[2] T. A. Chowdhury, M. A. B. Zafar, M. S.-U. Islam, M. Shahinuzzaman, M. A. Islam, and M. U. Khandaker, "Stability of perovskite solar cells: issues and prospects," *RSC Advances*, vol. 13, no. 3, pp. 1787–1810, 2023.

[3] F. Apadula, C. Cassardo, S. Ferrarese, D. Heltai, and A. Lanza, "Thirty years of atmospheric co2 observations at the plateau rosa station, italy," *Atmosphere*, vol. 10, no. 7, p. 418, 2019.

[4] M. A. B. Zafar, M. S.-U. Islam, M. R. Islam, and M. Shafiullah, "Optimized waste to energy technology combined with pv-wind-diesel for halishahar in chattogram," in *2022 IEEE International Conference on Electronics, Computing and Communication Technologies (CONECCT)*. IEEE, 2022, pp. 1–5.

[5] J. Dulout, B. Jammes, C. Alonso, A. Anvari-Moghaddam, A. Luna, and J. M. Guerrero, "Optimal sizing of a lithium battery energy storage system for grid-connected photovoltaic systems," in *2017 ieee second international conference on dc microgrids (icdcm)*. IEEE, 2017, pp. 582–587.

[6] J. Patel and G. Sharma, "Modeling and simulation of solar photovoltaic module using matlab/simulink," *International Journal of Research in Engineering and Technology*, vol. 2, no. 3, pp. 225–228, 2013.

[7] "Revista técnica bilingüe de energía," Jun 2022. [Online]. Available: https://futurenergyweb.es/

[8] M. Javidsharifi, H. Pourroshanfekr, T. Kerekes, D. Sera, S. Spataru, and J. M. Guerrero, "Optimum sizing of photovoltaic and energy storage systems for powering green base stations in cellular networks," *Energies*, vol. 14, no. 7, p. 1895, 2021.

[9] C.-H. Li, X.-J. Zhu, G.-Y. Cao, S. Sui, and M.-R. Hu, "Dynamic modeling and sizing optimization of stand-alone photovoltaic power systems using hybrid energy storage technology," *Renewable energy*, vol. 34, no. 3, pp. 815–826, 2009.

[10] B. Yodwong, D. Guilbert, M. Phattanasak, W. Kaewmanee, M. Hinaje, and G. Vitale, "Faraday's efficiency modeling of a proton exchange membrane electrolyzer based on experimental data," *Energies*, vol. 13, no. 18, p. 4792, 2020.

[11] J. Larminie, A. Dicks, and M. S. McDonald, *Fuel cell systems explained*. J. Wiley Chichester, UK, 2003, vol. 2.

[12] M. Gharibi and A. Askarzadeh, "Size and power exchange optimization of a grid-connected diesel generator-photovoltaic-fuel cell hybrid energy system considering reliability, cost and renewability," *International Journal of Hydrogen Energy*, vol. 44, no. 47, pp. 25 428–25 441, 2019.

[13] "Renewable power generation costs in 2020." [Online]. Available: https://www.irena.org/-/media/Files/IRENA/Agency/Publication/2021/Jun/IRENA_Power_Generation_Costs_2020_Summary.pdf

[14] I. Kumar, W. E. Tyner, and K. C. Sinha, "Input–output life cycle environmental assessment of greenhouse gas emissions from utility scale wind energy in the united states," *Energy Policy*, vol. 89, pp. 294–301, 2016.

[15] NASA, "National Aeronautics and Space Administration POWER — Data Access Viewer." [Online]. Available: https://power.larc.nasa.gov/data-access-viewer/